J. Ocean Univ. China (Oceanic and Coastal Sea Research)
https://doi.org/10.1007/s11802-019-3724-x
ISSN 1672-5182, 2019 18 (2): 394-402
http://www.ouc.edu.cn/xbywb/
E-mail:xbywb@ouc.edu.cn

A Localization Algorithm Using a Mobile Anchor Node Based on Region Determination in Underwater Wireless Sensor Networks

XU Tingting, WANG Jingjing*, SHI Wei, WANG Jianfeng, and CHEN Zhe

School of Information Science and Technology, *Qingdao University of Science and Technology*, *Qingdao* 266061, *China*

(Received November 13, 2017; revised June 15, 2018; accepted July 10, 2018)

Abstract At present, most underwater positioning algorithms improve the positioning accuracy by increasing the number of anchor nodes which resulting in the increasing energy consumption. To solve this problem, the paper proposes a localization algorithm assisted by mobile anchor node and based on region determination (LMRD), which not only improves the positioning accuracy of nodes positioning but also reduces the energy consumption. This algorithm is divided into two stages: region determination stage and location positioning stage. In the region determination stage, the target region is divided into several sub-regions by the region division strategy with the smallest overlap rate which can reduce the number of virtual anchor nodes and lock the target node to a sub-region, and then through the planning of mobile nodes to optimize the travel path, reduce the moving distance, and reduce system energy consumption. In the location positioning stage, the target node location can be calculated using the HILBERT path planning and trilateration. The simulation results show that the proposed algorithm can improve the positioning accuracy when the energy consumption is reduced.

Key words UWSN; mobile anchor nodes; energy consumption; region determination; localization algorithm

1 Introduction

With the increasing emphasis on the ocean and the rapid development of wireless sensor network research, the research of Underwater Wireless Sensor Networks (UWSN) has been paid more and more attention, while the key to underwater research is the accurate position of underwater target. Nowadays, underwater localization (Guo *et al.*, 2016) is always based on the acoustic signal with many disadvantages, such as large noise (Huang *et al.*, 2016), low speed, limited bandwidth, multipath effect and Doppler frequency shift (Li *et al.*, 2008; Stojanovic and Preisig, 2009). The anchor node is difficult to lay out (Zheng *et al.*, 2016) and restricted to carrying energy. The existing underwater localization system is characterized by low positioning accuracy and high energy consumption *etc*. In order to meet the high-precision and low-power positioning, this paper proposes a new positioning method.

The anchor node can be divided into fixed anchor node and mobile anchor node (MA) according to the anchor node can move or not. Fixed anchor nodes are generally laid by manual work or vessels and their position is determined by the laying device and the environment, such as density of water, and air viscosity coefficient (Lv, 2015). Mobile anchor nodes can be underwater drift nodes and high-speed motorized aircraft *etc*. Once known their own position, mobile anchor nodes can move regularly. After the mobile anchor node moves to the planned position and transmits the signal, it continues to move to the next planned position. All the planned positions are called virtual anchor nodes. Compared with fixed anchor nodes, mobile anchor nodes can avoid the laying difficulty and waste of resources during the recycling which bring the higher accuracy of location. The mobile anchor node, as an underwater wireless sensor network node, is equipped with Global Positioning System (GPS) navigation, which can effectively reduce the number of high-cost anchor nodes and reduce the cost of underwater operations greatly (Liao *et al.*, 2015). In order to solve the problem of underwater anchor nodes, such as laying out, energy consumption and the difficulties of energy supply, the autonomous underwater vehicle (AUV) is necessary for the underwater application of mobile anchor nodes (Carlson *et al.*, 2006; Guler *et al.*, 2017). But the AUV still needs to improve its underwater running time and depth control level to meet the requirements of the underwater environment. In order to make the AUV run a long time underwater, Townsend and Shenoi (2016) proposed a gyro wave energy purification system. For depth

* Corresponding author. Tel: 0086-532-88959279
E-mail: kathy1003@163.com

control, Claus and Bachmayer (2016) proposed a hybrid optimal energy depth controller to improve the control of the deployment depth for node. For optimal trajectory tracking control problem, Yang *et al*. (2016) proposed an approximate optimal tracking control (AOTC) approach. For security issues, Wang and Wang (2016) designed the active distributed antenna elements (DAE) set for orthogonal frequency-division multiplexing (OFDM) modulation and solved eavesdropper problem in the multi-point transmission. In the case of long-term monitoring a region, Allotta *et al*. (2016) proposed group AUV cooperative navigation and its absolute positioning error was close to GPS accuracy. In conclusion, AUV can meet people's needs for the function of mobile anchor nodes in depth control and security issues. And, it can extend the applications of sensor networks (Xu *et al.*, 2017; Dang *et al.*, 2017; Xu *et al.*, 2017; Xu *et al.*, 2017) from land to underwater.

The earliest applications of mobile anchor node location were in 2004 when Sichitiu ML (Han *et al.*, 2016) combined a single mobile anchor node and the ranging of received signal strength indicator (RSSI) to estimate the location of the target node. For the applications of mobile anchor node in static models, Alomari *et al*. (2017) proposed H-curves, which can achieve higher positioning accuracy and lower energy consumption in the determined environment. For the path planning of mobile anchor nodes, Koutsonikolas *et al*. (2006) proposed the SCAN, DOUBLESCAN and HILBERT for the first time according to the space filling line theory, but three methods had the collinear problem in different degrees. In order to effectively solve the problem, Huang *et al*. (2007) proposed circular path planning and S-shaped path planning two methods. Hence, based on trilateration algorithm, Han *et al*. (2013) introduced the localization with a mobile anchor node (LMAT) to optimize the motion trajectory of the mobile anchor node, which made the mobile anchor node monitor the target area according to the regular triangle trajectory and maximized the target positioning coverage and the positioning accuracy of the target node. 'S' type (Chen *et al*., 2012) reduced the total path length and prolonger the service life of the mobile anchor node. For the three-dimensional locating region, Liu *et al*. (2013) proposed the Hexahedral localization (HL) method, but this method had the high complexity. Due to the harsh conditions of ocean, localization for drifting restricted floating (LDSN) (Luo *et al*., 2016) uses buoys to meet the needs of positioning, where lacking anchor nodes for long-term maritime surveillance monitoring tasks. An asynchronous localization algorithm (Yan *et al*., 2017) eliminates the influence of asynchronous clock by iterative least squares estimator and compensates the mobility of sensor node. Luo *et al*. (2017) leverage nodes' restricted movement to realize three-dimensional sensor networks underwater for sustainable monitoring tasks. The extended Kalman filter (EKF) model realizes the real-time positioning of the system by considering the motion of the AUV which improves the positioning accuracy of the traditional Long Baseline (LBL). That the target node receives enough virtual anchor node information and the number of the reference nodes meets the needs is a question. In the above-mentioned positioning algorithm based on the mobile anchor node, the adjacent virtual anchor nodes have overlapping coverage in order to solve the question. That not only lengthens the MA's path length but also increases the energy consumption of positioning.

Reducing the energy consumption of an underwater positioning system remains the biggest issue. To solve this problem, one way is to reduce the number of virtual anchor nodes. However, reducing the number of virtual anchor nodes blindly will seriously affect the positioning accuracy based on mobile anchor nodes. To this end，this paper proposes LMRD algorithm. The LMRD algorithm improves the positioning accuracy of nodes as well as reducing the energy consumption. The following contributions are made in this paper:

a) The shape of the sub-regions was defined, a hexagon, which reduce coverage overlap areas of virtual anchor nodes. HILBERT was chosen as path planning within the sub-region and the number of virtual anchor nodes was increased to improve the positioning accuracy.

b) The path planning between sub-regions were defined. Compared with SCAN, the MA's path length and the energy consumption could be reduced.

c) Extensive simulations were conducted to validate and evaluate our proposed algorithm. The simulations proved the efficiency and effectiveness of our proposed algorithm.

The rest of the paper is structured as follows: Section 2 describes the proposed localization algorithm LMRD in detail. Based on positioning accuracy, energy consumption and positioning time, this paper compares the performance of the LMRD with the traditional localization algorithm in Section 3. At last Section 4 concludes the paper.

2 Design of UWSN Location Algorithm Based on Mobile Anchor Node

The LMRD algorithm is divided into two stages, namely, the region determination stage and the location positioning stage. The target area is divided into a plurality of sub-regions *Qi* in the region determination stage. The sub-region *Qb*, where the target node is located in, is positioned by the anchor nodes moving quickly. The entire target area is required to be completely covered by all sub-regions, but the overlapping area is minimized. In the location positioning stage, when the sub-region *Qb* was known, the position of the target node can be obtained by using the intersection of the three circles of the trimming method. In the region determination stage, only the location of sub-region *Qb* is needed to determine, so that the accuracy requirements are low and the number of virtual anchor nodes required is small, which reduces the energy consumption. In the location positioning stage, the number of virtual anchor nodes is needed to increase to achieve the purpose of improving the location accuracy.

2.1 Regional Division Strategy

During the movement of the anchor node, the main energy consumption is derived from the virtual anchor node transmitting signal and its own motion, and the signal transmission consumes most energy. In order to extend the working time of the anchor nodes, the number of mobile anchor nodes transmitting signals should be minimized in the course of movement. In the region determination, the target area is needed to be covered by virtual anchor nodes completely, and the area covered by each virtual anchor node is a circle with a radius known. Therefore, in order to reduce the number of anchor nodes transmitting signal, two regional division strategies are adopted: strategy one, the shape of the sub-regions in the target area can be completely stitched. Strategy two, the area of the sub-region is approximately equal to the area of a circle.

In order to cover the target area completely, the shape of the sub-region *Qi* may be a regular triangle, a square and a regular hexagon, as is shown in Fig.1. Assuming that the radius of the circle is R, and its area is $S=\pi\times R^2$, the square side length is $\sqrt{2}\times R$, then the area is $S=\pi\times R^2$, the height of the triangle is high $H=3/2\times R$, the length is $\sqrt{2}\times R$, then the area is $S_2=3\sqrt{3}\times R^2/4$. The length of the regular hexagon is R, the area is

$$S_3=6\times\frac{1}{2}\times\frac{\sqrt{3}}{2}\times R^2=3\sqrt{3}\times R^2/2.$$

The results are shown as Table 1. From Table 1, it is clear that $S_3>S_1>S_2$, $S_3/S=3\sqrt{3}/2\times\pi$, the overlapping area of each two sub-region is

$$S_\Delta=\frac{2\pi-3\sqrt{3}}{12}\times R^2\approx 0.09R^2.$$

Table 1 Comparison of sub-region

Parameter	Length	Area	Ratio of the circular area
Triangle	$\sqrt{3}\times R$	$3\sqrt{3}\times R^2/4$	$3\sqrt{3}/4\times\pi$
Square	$\sqrt{2}\times R$	$2\times R^2$	$2/\pi$
Hexagon	R	$3\sqrt{3}\times R^2/4$	$3\sqrt{3}/2\times\pi$

It is clear that the area of the regular hexagon is close to the area of the circle, as Fig.1. According to the regional division strategy, the optimal sub-region is the regular hexagon.

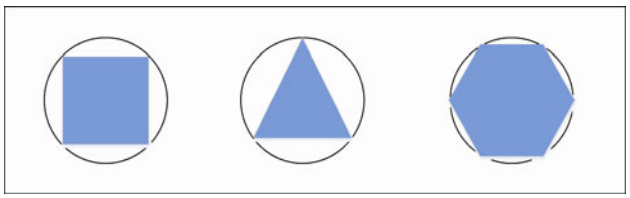

Fig.1 Comparison of area occupied by polygons in the same circle.

2.2 Planning Route and Motion Mechanism of Mobile Anchor

In the whole process of localization, the movement of the anchor node is divided into two stages, the region determination stage and the location positioning stage respectively. During the first stage, the motion range of the anchor node is the whole target area, which requires the anchor node to traverse the hexagonal sub-regions in turn until it receives the feedback information. The movement range of the second stage is a hexagonal sub-region, which is the result of the region determination and the basis of the localization, and the number of virtual anchor nodes is increased in order to position precisely. Obviously, the MA only needs to satisfy that all the virtual anchor nodes are covered completely in the first stage. In order to reduce the energy consumption of MA, the length of the moving path of the MA must be reduced.

The LMAT requires the mobile anchor node travelling the monitoring area following a regular triangle trajectory, so as to achieve maximum positioning coverage and high localization accuracy. Anchor points compose regular triangles to insure the localization accuracy, as depicted in Fig.2. The mobile anchor node broadcasts the acoustic signal periodically at the virtual anchor node during the movement, which includes information such as timestamp and current position. The main advantage of LMAT is to solve the collinearity problem.

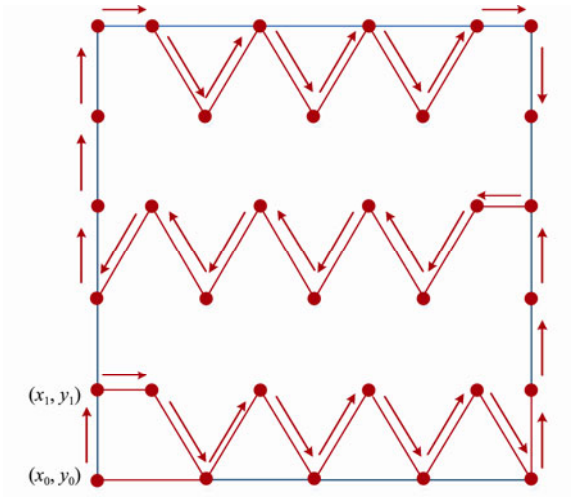

Fig.2 Path planning of LMAT.

Though optimizing the distribution of the virtual anchor nodes (as is shown in Fig.3), the ‘S’ type path planning improves the movement efficiency, reduce the total path length and extend the lifetime of the mobile anchor node. The authors use an ‘S’ type as macro movement trajectory for mobile anchor node. The unknown nodes can receive four uniformly distributed data packets in a small square area, reducing the problem of collinearity.

However, the goal of LMAT is to improve the localization accuracy, but the energy consumption and path length of the mobile anchor nodes are not considered in this process. 'S' type reduces the total path length of the mobile anchor nodes, but the overlap areas still cause an increase in energy consumption. To this end, LMRD algorithm is proposed in this paper which can minimize the coverage overlap areas of virtual anchor nodes and reduce energy consumption.

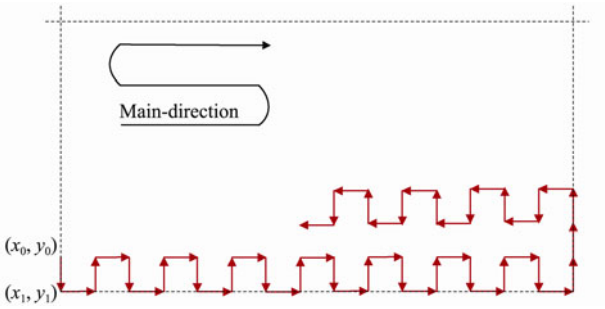

Fig.3 Path planning of 'S' type.

As is shown in Fig.4, it is assumed that the radius of the circle is R and MA traverses using the shown route, where the dotted lines indicate the boundaries of the target area. As Fig.4 (a), the length of moving path is

$$L_a = \sqrt{3} \times R \times 11 \times 7 = 77\sqrt{3}R. . \quad (1)$$

As Fig.4 (b), the length of moving path is

$$L_a = \sqrt{3} \times R \times 11 \times (\sqrt{3} \times R + 9 \times 3R) \times 7 = 7\sqrt{3}R + 189R. . \quad (2)$$

Then $L_b - L_a = 189R - 70\sqrt{3}R = 67.8R \approx \frac{1}{2}L_a$.

It can be seen that the length of route in Fig.4 (a) is only half of that as Fig.4 (b). To reduce the operation time and energy consumption, the moving path shown as Fig.4 (a) is chosen.

When there is only one mobile anchor node in the target area, it is necessary to design its movement between the two stages, and to ensure that the mobile anchor node can reach the virtual anchor node position (such as the point M in Fig.4) quickly in location positioning stage. It is assumed that the coverage radius of the anchor node R is 200 meters, and the speed of sound in the water is 1500m/s, and the time interval of target node between the signal receiving and the transmitting feedback signal is t_0, and the maximum time interval of MA receiving the feedback signal is $0.267S + t_0$. The moving speed of the mobile anchor node is 5m/s, and the position of the virtual anchor node can be obtained by the time t of the MA's movement. The fastest reaching route can be designed by changing the direction and manner of the anchor nodes.

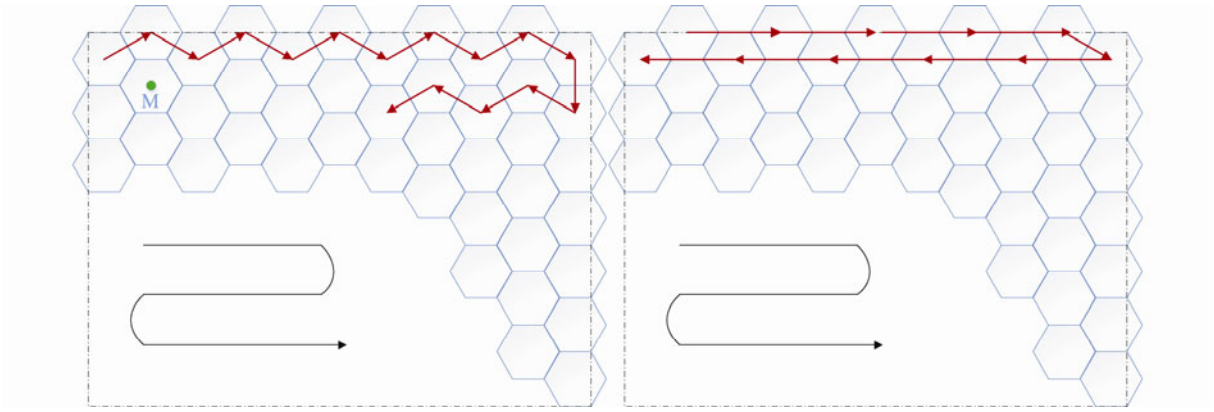

Fig.4 Moving path of MA in the region determination.

2.3 Region Determination

The mobile anchor node is equipped with GPS navigation, which can get its accurate position on the water surface by radio waves. In order to obtain the exact absolute position of the virtual anchor node, the mobile anchor node dive to the specified depth after reaching the exact position. When the preset position is reached, the mobile anchor node starts broadcasting information to the surroundings, including its location information, timestamp information, and so on. After broadcasting information, the mobile anchor node adjusts its operating angle and moves to the next virtual anchor node. During this process, the mobile anchor node no longer broadcasts the information, but can still receive the information. After the target node receives and confirms the information of the mobile anchor node, it sends the feedback information to the mobile anchor node, such as confirmation information and timestamp information. After the mobile anchor node receives the feedback information, the area Qb where the target node is located can be determined.

Since the area of each sub-region Q is smaller than the coverage of the virtual anchor node in the region determination, the situation shown as Fig.5 will emerge. Ideally, the position of the target node is judged into the Qb_2 area. But target node is judged into the area Qb_1 in the actual operation. This situation needs to be corrected for whether the region determination is correct determines the accuracy of the position determination. After the mobile anchor node receives the first feedback, it is judged whether or not the area node P needs to perform the area determination again. According to the feedback informa-

tion received, the mobile anchor node can measure the distance between the virtual anchor node and P. If the range of the distance d is among $\left(\sqrt{3}/2R, R\right)$, and R is the coverage radius of the MA, then a new route will be planned to ensure the correctness of the region determination.

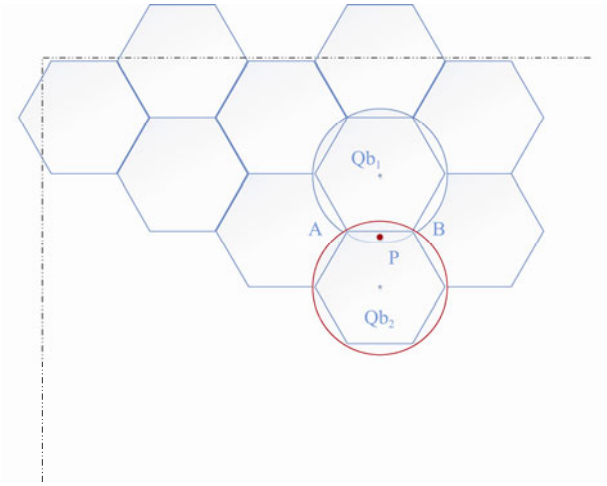

Fig.5 First region determination.

When a new route is designed, the mobile anchor node just needs move around the original virtual anchor node, since the target node P must be near the original virtual anchor node. As is shown in Fig.6, there is only the area where the virtual anchor nodes N and O are not reached, adjacent to the area Qb_1.After the mobile anchor node arrives at M, it will move to the virtual anchor node N according to the preset trajectory. After reaching N, MA moves to O. If the mobile anchor node arrives at O, it does not receive the feedback information of the target node P, and then the mobile anchor node will move to the original virtual anchor node M. If the MA receives the feedback information of the target node near O or N and the measured distances OP' and NP' is between $\left(0, \sqrt{3}/2R\right)$, the area of the target node is determined as the area where O or N is located, otherwise the area is Qb_1.

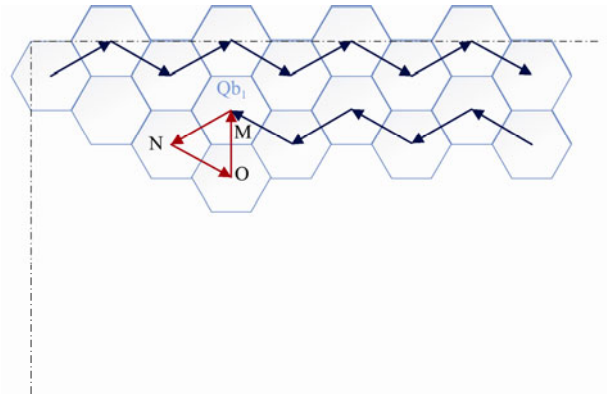

Fig.6 Path planning to region determination again.

2.4 Location Positioning

The goal of UWSN node positioning is to obtain the location of the target node. But now the target node location is just limited to a sub-region, and the further location positioning is needed. The range of the sub-region is the hexagon centered on the virtual anchor node. In order to complete the scanning of all the virtual anchor nodes quickly and with energy-saving in the region *Qb*, HILBERT curve (as is shown in Fig.7) is used as the path planning of location positioning. At the same time, the number of mobile anchor nodes and collinearity problem are taken into account.

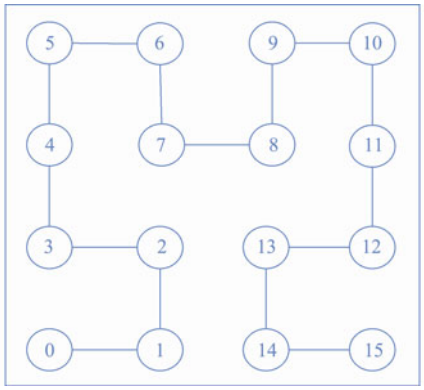

Fig.7 Path planning of HILBERT.

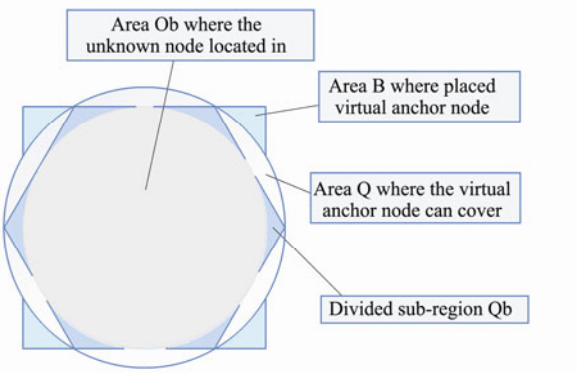

Fig.8 Comparison of Qb and coverage areas of HILBERT.

Since the HILBERT curve is planned in the square area and the sub-region is a regular hexagon, it is necessary to consider whether the region Qb can be completely covered and the number of signals that can receive from the reference node. The target node uses the trilateration to calculate the coordinates, so it is necessary to receive signals from at least three reference nodes to complete the positioning of the two-dimensional space. The depth information of the target node is self-test by the gravity sensor, that is to say, coordinate calculation of three-dimensional space can be reduced to two-dimensional space. As is shown in Fig.7, it is necessary to determine whether or not the target node is within the inscribed circle Qb' of the area B in the location positioning stage, that is to say, the position of the target node at area Qb' or Qb – Qb'. In the layout area, as is shown in Fig.8, it is clear that the target node in the region Qb' can be completely covered by the anchor node, and whether the target node within Qb– Qb' can be covered completely is uncertain, so the following analysis is required. As is shown in Fig.9, for the left tip region, it is clear that the anchor nodes at 3 and

4 can be completely covered by the virtual anchor nodes at 2 and 7. As can be seen from Fig.9, this area can receive signals from at least four reference nodes. Therefore, the information of the three reference nodes is used to calculate the coordinates of target node.

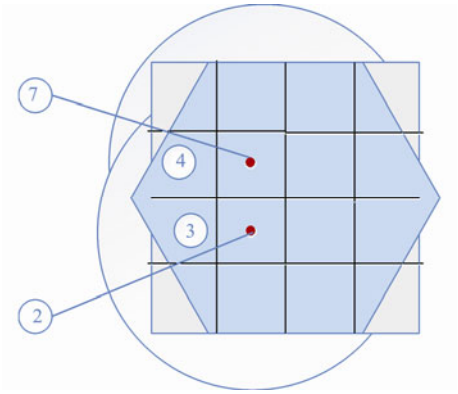

Fig.9 The node full coverage area confirmation in HILBERT curve.

The main process of the LMRD algorithm can be summarized as follows:

Input: *bi*, *R*, *Hbi*;
Output: *B*;
1 Initialize the searching range $r = 1000 \times 1000$ m and set the root b_0 as the start node;
2 **for** every beacon *bi* **do**
3 Calculate the distance of *bi* (*xi*, *yi*) and unknown node *B*(*x*, *y*), then select the coverage area *Q* of *bi* (*xi*, *yi*) as the possible area, which firstly satisfy

$$\sqrt{(x_i - x)^2 + (y_i - y)^2} < R;$$

4 **If** the distance of *bi* and

$$B\sqrt{(x_i - x)^2 + (y_i - y)^2} < \sqrt{3}/2R;$$

then the area Q_i is where the unknown node in;
else judge the other 2 possible beacons,
if the distance of bi and O or

$$N\sqrt{(x_i - x)^2 + (y_i - y)^2} < \sqrt{3}/2R,$$

then the area Q_0 or Q_n is where the unknown node in, when all the possible beacons do not meet the conditions, then *Q* is chosen as the result of Regional decision;
5 **end**
6 **for** every beacon *Hbi* of Q **do**
7 **if** the distance of *Hbi* (*xi*, *yi*) and unknown node *B*(*x*, *y*) less *R*, then let *Hbi* be the reference node of *B*, *k*=*k*+1;
8 **if** *k*>=4, sort the distance and select four near nodes as the basis of positioning and use LS to calculate the coordinate of *B*;
else if *k*=3, use trilateration to calculate the coordinate of *B*;
9 **end**
10 **Output** *B*

3 Results and Analysis

The LMRD was simulated using MATLAB. Set the positioning area as a 1000 m× 1000 m square area with linear FM signal (as is shown in Table 2) and the channel of Bellhop model.

Table 2 FM signal parameter settings

Frequency range (Hz)	Time length (s)	Sampling frequency (Hz)
[200, 300]	0.05	10000

In addition, the other environment variables are obtained from the formula Eq.(3), Eq.(4), Eq.(5), and the specific values are shown as Table 3.

$$T = 7.5 + \frac{8.5}{700} \times (700 - depth), \quad (3)$$

where *T* is the temperature of the seawater, and depth is the distance between the node and sea level.

$$S = 34.2 + \frac{1.3}{1000} \times (1000 - depth), \quad (4)$$

where *S* is the salinity of the seawater.

Table 3 Environment variable settings

SNR (dB)	Acoustic speed (m/s)	Depth (m)	Temperature (℃)	Salinity
20dB	1508.1	100	14.1785	35.37

$$C = 1448.96 + 4.591 \times T - 5.304 \times 10^{-2} \times T^2 + 2.374 \times 10^{-4} \times T^3 + 1.340 \times (S - 35) + 1.630 \times 10^{-2} \times depth + 1.675 \times 10^{-7} \times depth^2 - 1.025 \times 10^{-2} \times T \times (S - 35) - 7.139 \times 10^{-13} \times T \times depth^3, \quad (5)$$

where *C* is the speed of the acoustic in seawater.

3.1 Process of Location Positioning

Simulation is carried out in the above environment. First, the area Qb where the target node is judged, and then the virtual anchor nodes are arranged in the region Qb according to the HILBERT curve. As is shown in Fig. 10, the green dot represents the location of the virtual anchor node for the region determination, and the red dot represents the location of the virtual anchor node positioned in the location positioning, and the red circle represents the result of regional decision, and the black circle represents the placement range of virtual anchor node which the target node can receive, and the blue point is the actual position of the target node (685.0630, 573.3153), and the purple point is the calculated target

node position (684.9018, 574.0807) with an error of 0.7822 m.

Fig.11 shows the statistics of the LMRD simulation in this environment. It can be obtained from the simulation results that the positioning error is in the majority of 1.5m or less, with the average error of 0.661 meters, and positioning accuracy can reach meters.

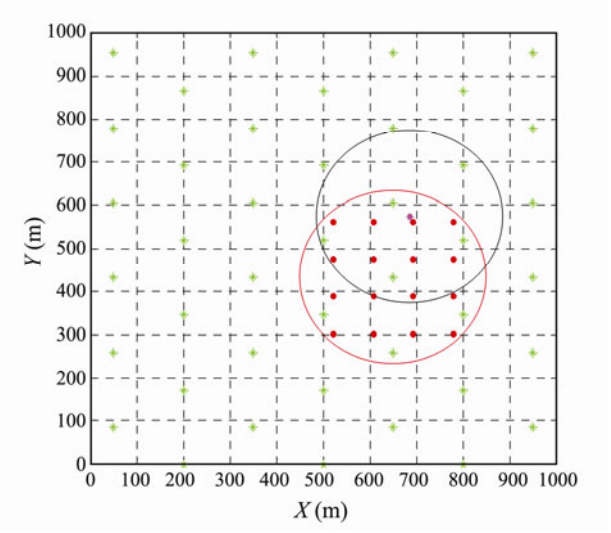

Fig.10 Positioning results.

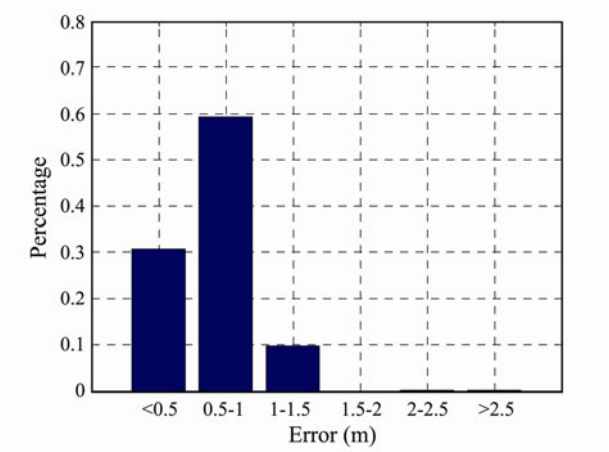

Fig.11 Statistics of 1000 simulation error results.

3.2 Analysis of Performance Comparison

It can be obtained from comparison of four algorithm results in Fig.12. Only 90% of the simulation error in the 'S' type and LMAT algorithms is within 1.2m, and 99% of the simulation error is within 1.7m. For HILBERT algorithm, 90% of the simulation error is within 1.2m, but the simulation error within 2 m is only 92%. For Circular algorithm, 84% of the simulation error is within 1.2m, but the simulation error within 2 m is only 95%. However, 99% of the simulation error is within 1.2m using LMRD.

According to Fig.13, the LMRD algorithm accuracy can reach the meter level without greater positioning error.

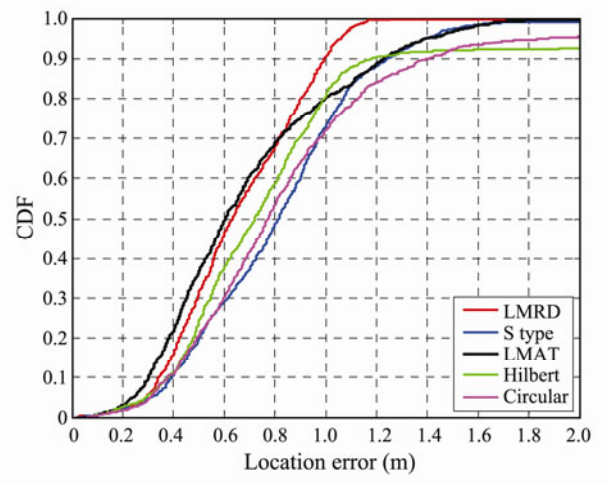

Fig.12 Comparison of cumulative distribution functions for error estimation.

In order to compare the energy consumption of the four positioning algorithms preferably, it is assumed that the position of the target node is located at the center of the selected region, and the coordinates are (500, 500). In LMRD algorithm, the coordinates of the virtual anchor node which first receives from the target node are (350, 433.01). The number of the virtual anchor nodes is 20 in region determination, which includes 17 virtual anchor nodes that receive the first feedback information and 3 virtual anchor nodes that need reconfirming. In the location positioning stage, the fixed number of virtual anchor nodes is 16.

Table 4 Comparison of the number of MA mobile paths and virtual anchor nodes

Parameter	'S' type	LMAT	HILBERT	Circular	LMRD algorithm
Quantity	64	44	56	64	36
Length (m)	8909.55	7685.64	9600	9424.78	4589.93

In Table 4, Length refers to the length of the path that the mobile anchor node moves, and Quantity means the number of virtual anchor nodes.

It can be obtained from comparison, the energy consumption of motion and broadcasting packets in traditional location algorithms is higher than that of the LMRD. And it can be proved that the LMRD can significantly reduce the energy consumption of localization. Because the moving speed of the mobile anchor node is low, and the length of the moving path of the MA determines the time required for the localization directly. It can be seen that the LMRD algorithm has a significant reduction in path length, and also has made a breakthrough in the positioning time.

4 Conclusions

Based on the region determination, the UWSN node location algorithm assisted by mobile anchor node was proposed in this paper. The shape of the sub-region was defined in the region determination and the overlapping area of the virtual anchor node was reduced. The path

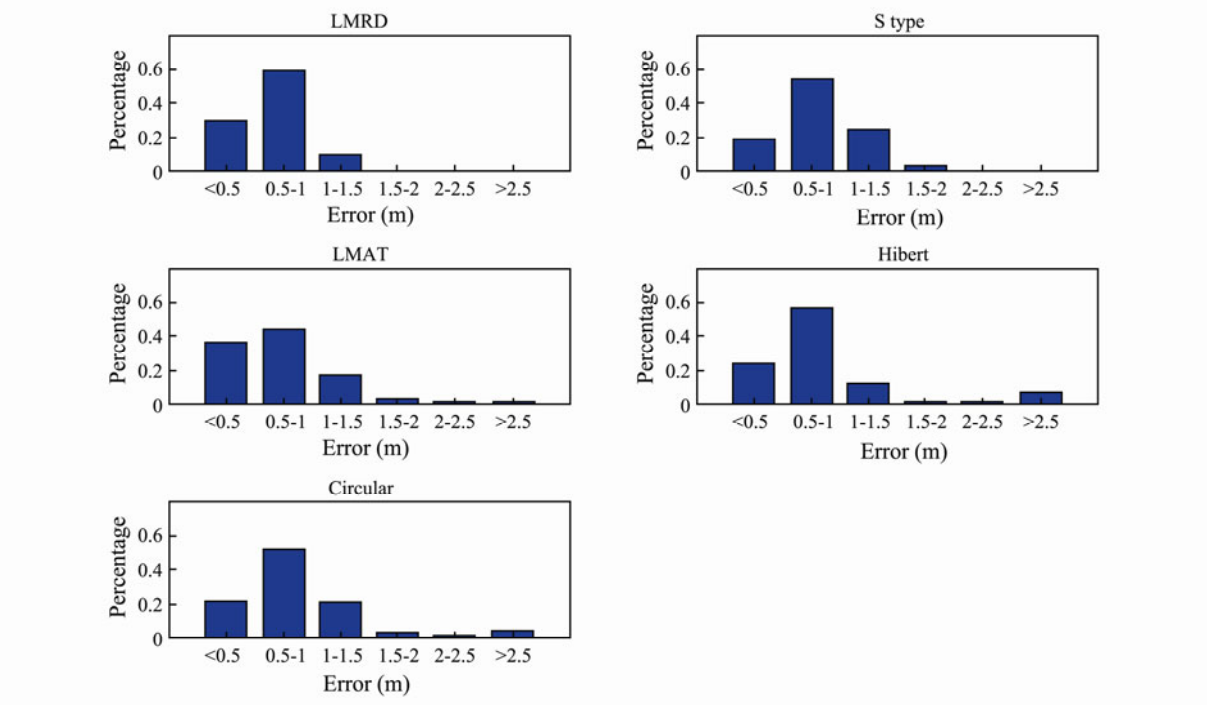

Fig.13 Comparison of error.

planning between regions was studied to reduce the path length and energy consumption of mobile anchor nodes. The accuracy of localization was determined by the location positioning stage in the sub-region. And the number of reference nodes can guarantee high localization accuracy, so the number of virtual anchor node was increased in sub-region relatively. In summary, on the basis of ensuring positioning accuracy, LMRD greatly reduces energy consumption and shortens positioning time. However, only the environmental factors such as wind speed and salinity were taken into account in this paper, and the factors such as noise and seawater flow during the movement of the anchor nodes were not considered. In the future, the test will be carried out in the actual environment to improve the LMRD algorithm.

Acknowledgments

The authors would like to thank the referees and editors for providing very helpful comments and suggestions.

This research was supported by National Natural Science Foundation of China (Nos. U1806201, 61671261), Key Research and Development Program of Shandong Province (No. 2016GGX101007), China Postdoctoral Science Foundation (No. 2017T100490), and University Science and Technology Planning Project of Shandong Province (Nos. J17KA058, J17KB154).

References

Guo, S. L., Tang, R. C., Peng, L. H., and Ji, X. P., 2016. Matched field localization based on CS-MUSIC algorithm. *Journal of Ocean University of China*, **15** (2): 254-260.

Huang, B., Ge, C., and Yong, H., 2016. Research on strategy marine noise map based on i4ocean platform: Constructing flow and key approach. *Journal of Ocean University of China*, **15** (1): 117-123.

Li, B., Zhou, S., Stojanovic, M., Freitag, L., and Willett, P., 2008. Multicarrier communication over underwater acoustic channels with nonuniform Doppler shifts. *IEEE Journal of Oceanic Engineering*, **33** (2): 198-209.

Stojanovic, M., and Preisig, J., 2009. Underwater acoustic communication channels: Propagation models and statistical characterization. *IEEE Communications Magazine*, **47** (1): 84-89.

Zheng, Z., Xu, J., Huang, P., Wang, L., Yang, X., and Chang, Z., 2016. Dynamics of anchor last deployment of submersible buoy system. *Journal of Ocean University of China*, **15** (1): 69-77.

Lv, X. B., 2015. *The Numerical Modeling Approach of an Air-Launched AUV Impacting into Water.* Harbin Engineering University Press, Harbin, 32pp (in Chinese).

Liao, W. H., Lee, Y. C., and Kedia, S. P., 2011. Mobile anchor positioning for wireless sensor networks. *Iet Communications*, **5** (7): 914-921.

Carlson, E. A., Beaujean, P. P., and An, E., 2006. Location-aware routing protocol for underwater acoustic networks. *Journal of Electrical & Computer Engineering*, **2012** (2): 1-6.

Guler, S., Fidan, B., Dasgupta, S., Anderson, B. D. O., and Shames, I., 2017. Adaptive source localization based station keeping of autonomous vehicles. *IEEE Transactions on Automatic Control*, **62** (7): 3122-3135.

Townsend, N. C., and Shenoi, R. A., 2016. Feasibility study of a new energy scavenging system for an autonomous underwater vehicle. *Autonomous Robots*, **40** (6): 1-13.

Claus, B., and Bachmayer, R., 2016. Energy optimal depth control for long range underwater vehicles with applications to a hybrid underwater glider. *Autonomous Robots*, **40** (7): 1307-1320.

Yang, Q., Su, H., and Tang, G., 2016. Approximate optimal tracking control for near-surface AUVs with wave distur-

bances. *Journal of Ocean University of China*, **15** (5): 789-798.

Wang, C., and Wang, Z., 2016. Signal alignment for secure underwater coordinated multipoint transmissions. *IEEE Transactions on Signal Processing*, **64** (23): 6360-6374.

Allotta, B., Caiti, A., Costanzi, R., Costanzi, R., Corato, F. D., and Fenucci, D., 2016. Cooperative navigation of AUVs via acoustic communication networking: Field experience with the Typhoon vehicles. *Autonomous Robots*, **40** (7): 1229-1244.

Xu, L., and Gulliver, T. A., 2017.Performance analysis for m2m video transmission cooperative networks using transmit antenna selection. *Multimedia Tools & Applications*, **76** (22): 23891-23902.

Dang, S., Chen, G., and Coon, J. P., 2017. Outage performance analysis of full-duplex relay-assisted device-to-device systems in uplink cellular networks. *IEEE Transactions on Vehicular Technology*, **66** (5): 4506-4510.

Xu, L., Wang, J., Zhang, H., and Gulliver, T. A., 2017. Performance analysis of IAF relaying mobile D2D cooperative networks. *Journal of the Franklin Institute*, **354** (2): 902-916.

Xu, L., Zhang, H., Wang, J., and Gulliver, T. A., 2017. Joint TAS/SC and power allocation for IAF relaying D2D cooperative networks. *Wireless Networks*, **23** (7): 2135-2143.

Han, G., Jiang, J., Zhang, C., Duong, T. Q., and Guizani, M., 2016. A Survey on mobile anchor node assisted localization in wireless sensor networks. *IEEE Communications Surveys & Tutorials*, **18** (3): 2220-2243.

Alomari, A., Comeau, F., Phillips, W., and Aslam, N., 2017. New path planning model for mobile anchor-assisted localization in wireless sensor networks. *Wireless Networks*, 1-19.

Koutsonikolas, D., Das, S. M., and Hu, Y. C, 2006. Path planning of mobile landmarks for localization in wireless sensor networks. *Computer Communications*, Lisboa, Portugal, Portugal, **30** (13): 2577-2592.

Huang, R., and Zaruba, G. V., 2007. Static path planning for mobile beacons to localize sensor networks. *IEEE International Conference on Pervasive Computing and Communications Workshops*, White Plains, NY, USA, 323-330.

Han, G., Xu, H., Jiang, J., Shu, L., and Hara, T., 2013. Path planning using a mobile anchor node based on trilateration in wireless sensor networks. *Wireless Communications & Mobile Computing*, **13** (14): 1324-1336.

Chen, H., Liu, B., Huang, P., Liang, J., and Gu, Y., 2012. Mobility-assisted node localization based on TOA measurements without time synchronization in wireless sensor networks. *Mobile Networks & Applications*, **17** (1): 90-99.

Liu, L., Zhang, H., Geng, X., and Shu, X., 2013. Hexahedral localization (HL): A three-dimensional hexahedron localization based on mobile beacons. *The Scientific World Journal*, **2013** (5): 1-11.

Luo, H., Wu, K., Gong, Y., and Ni, L., 2016. Localization for drifting restricted floating ocean sensor networks. *IEEE Transactions on Vehicular Technology*, **65** (12): 9968-9981.

Yan, J., Zhang, X., Luo, X., Wang, Y., Chen, C., and Guan, X., 2017. Asynchronous localization with mobility prediction for underwater acoustic sensor networks. *IEEE Transactions on Vehicular Technology*, **67** (3): 2543-2556.

Luo, H., Wu, K., and Hong, F., 2017. Ocean Barrier: A floating intrusion detection ocean sensor networks. *International Conference on Mobile Ad-Hoc and Sensor Networks*, Hefei, China, 390-394.

Zhang, J., Shi, C., Sun, D., and Han, Y., 2018. High-precision, limited-beacon-aided AUV localization algorithm. *Ocean Engineering*, **149** (1): 106-112.

(Edited by Ji Dechun)